Motion of waves in shallow water

Interaction between waves and sand bottoms

By R. A. Bagnold, F.R.S.

(*Received* 14 *August* 1945—*Read* 31 *January* 1946)

With an additional note by Sir Geoffrey Taylor, F.R.S.

[Plates 1–4]

The loss of energy of a travelling water wave, due to the mechanism of the formation of sand ripples and water vortices on a sandy bed, becomes of practical importance when models are used to predict full-scale foreshore movements.

On the assumption that the bottom-water oscillation is nearly simply harmonic, the mechanism was studied by oscillating a section of bed through still water.

The pitch, p, of the sand ripple formed was found to vary as the square root of the grain diameter, independently of the speed and of the grain density, for amplitudes, R, of water motion exceeding this pitch. But for smaller amplitudes the pitch shortens with decreasing amplitude of movement.

The mean drag coefficient, k, in the case of artificial rigid ripples, was measured directly. For R/p less than unity, k remains constant. For R/p greater than unity, k was found to vary as $(R/p)^{-0\cdot75}$. These results are compared with the case of steady flow.

The critical water speeds and amplitudes for first disturbance of grains on a smoothed surface was also measured, over a wide range of grain diameters and densities. The results conform closely to a simple empirical expression.

1. Introduction

The success of many major maritime engineering projects depends on the correct prediction of the movement of the bottom under the action of waves. Were the laws known which govern the interaction between the bed material and the oscillating motion of the water in contact with it, the use of models would be of far greater help than is at present the case. For though model waves over a smooth rigid bed run remarkably true to scale, serious discrepancies occur when one tries to imitate their effect on loose granular bed material. The quantity of sand transported is too little; the area where the bed is active is too restricted; and the bed is corrugated with ripples of a size out of all proportion to their full-scale prototypes. These comparatively big ripples make the drag between the bed and the water too great, and the waves become exhausted too soon.

The object of the experiments to be described was to obtain quantitative data (*a*) on the size and character of the sand ripples made by waves, (*b*) on the drag to which these ripples give rise, and (*c*) on the minimum oscillating water motion required to disturb the sand in the first instance.

The experiments were confined to the simplest case of a continuous train of symmetrical waves travelling over a horizontal bed. They are intended as a first instalment of a research into the movement of sand by water motions in which wave action predominates.

2. Bottom-water motion

Classical wave theory, though it neglects drag, was assumed to give with sufficient accuracy the water motion near the bottom. For waves in deep water and also for those shallow-water waves in which the wave height is small compared with the depth, the horizontal oscillations of the water near the bottom are known to approximate closely to simple harmonic motion. For shallow-water waves of extreme height a connected train of solitary waves of greatest height may be taken, as worked out by McCowan (1891). Here, too, when a suitable steady reverse motion is superimposed on the whole body of the water in order to approximate to the practical case of a channel of finite length, the remaining motion at the bottom deviates surprisingly little from simple harmonic. It is only when the repetition distance exceeds the 'wave-length' $2\pi/m$ that large deviations occur. The horizontal acceleration at the bottom appears never to exceed $g/6$ provided the wave is steady.

Hence simple harmonic bottom-water motion of amplitudes less than $g/6\omega^2$ (where the angular velocity $\omega = 2\pi/\text{wave period}$) appears to cover a wide range of practical conditions.

3. Nature of the experiments to be described

In view of the above it was felt that the results of observations, made far more conveniently by oscillating the bottom harmonically through still water, would not differ appreciably from the real effects on a still bottom produced by water motion provided the accelerating form on the grains via the bed, due to the driving mechanism, is small compared with the fluid force acting on them. All the results given and discussed in this paper have been obtained in still water.

The two sets of experiments were carried out between October 1944 and February 1945 in the hydraulics laboratory at Imperial College with the help of Dr C. M. White.

In experiment 1, in which was observed the behaviour of actual sands, the sand was contained in a cradle suspended from a pivot in the roof so that it could be oscillated through a circular arc in still water in a narrow tank. (Incidentally, this tank happened by chance to be one of those used years ago by Mrs Ayrton for her qualitative study of water-sand ripples.) The oscillation was maintained by means of a motor-driven crank, as shown in figure 5*a*, plate 1.

For each of a range of different semi-amplitudes R, from 25 to 0·5 cm., a series of runs were made at different angular speeds ω, increasing from the lowest speed at which each sand began to move over the bed, up to the point at which the acceleration of the cradle at the end of the stroke reached such a value $\mu g \dfrac{(\sigma-\rho)}{\sigma}$ that the whole sand mass started sliding on the steel cradle-floor. Between these limits a wide range of ripple phenomena was observed.

In experiment 2 (figure 5*b*, plate 1), by which the ripple drag was measured, a celluloid plate, of submerged dimensions 1 m. long and 50 cm. deep, to which fixed imitation ripples were attached, was hung vertically in a large tank of water from a horizontal runway. The plate was oscillated by the same driving mechanism, from which, however, the motor was disconnected and replaced by a winding drum and a wire to which weights could be hung.

This apparatus, motor driven, was also used to take still and cine-pictures of the water motion near the plate, as indicated on the free surface by a scattering of aluminium powder. The cameras were mounted on the plate carriage and moved with it.

4. General observations on the water motion over the ripple

In figure 6, plate 2, where R was 20 cm., the ripple pitch p, 10 cm. and ripple height h (trough to crest), 1·5 cm., the phase of the stroke in which each exposure was made is indicated by the pointer, end of stroke being at the bottom. The series shows one stroke (half a completed oscillation) during which the pointer rotated anti-clockwise through a complete revolution, the ripple (and camera) moved to the left and the main water-mass to the right.

In interpreting the series it should be remembered that the camera moved with the ripples, and though the small eddies within the ripple trough and travelling with it appear sharply in each photograph, the large free vortices are only visible clearly as such when they happen to be at rest relatively to the camera, i.e. at the end of the stroke. They are, however, there all the time, and their ghosts can be distinguished by the waviness of the particle streaks.

The water motion differs according as the stroke length $2R$ is greater or less than the ripple pitch p (crest to crest). If it is greater (high mid-stroke velocities and low end-stroke accelerations), the trough is occupied during most of the stroke by small eddies which have developed from the lee crest, and we seem to have the beginnings of successive true, though incipient, stead-flow boundary layers. For strokes many ripples in length the little eddies may grow, break up and drift away and be replaced by others several times before the stroke ends.

But as the stroke is shortened, the formation of the eddies inside the troughs is delayed till a later and later phase, and when $2R$ is less than p the troughs are empty of eddies till the last quarter is reached.

During retardation at the end of the last quarter of the stroke, a single eddy in the middle of the trough rapidly grows into a very large vortex, which fills the whole trough. At the end of the stroke, or in the case of very short strokes at the beginning of the next return stroke, its inertia causes the vortex to lag behind, so that it leaves the middle of its trough and mounts up the slope past the crest and out into free water. During successive subsequent strokes it is forced farther and farther outwards away from the surface as new vortices are formed and ejected after it. In the first photograph the vortex appearing centrally over the ripple crest is an old one ejected at the end of the previous stroke. The remains of older ones can also be seen farther out. The general outward drift of the vortices produces a slow cellular circulation in the mass of the water, which extends to a great distance from the ripple surface; and if the terminal velocity of fall of the sand grains is slow, the vortices carry up curtains of suspended grains with them.

Time has not allowed of a detailed study of the effect on the water motion of varying the shape of the ripple section. In the artificial fixed ripples used, the ratio of wave-length to height was 6·7. It will be apparent from what follows that the big end-of-stroke ripple vortex will not form if this ratio is much increased. The formation of the ripple vortex seems to be confined to oscillatory motion, and there is no evidence for the existence of vortices of such a size under conditions of steady flow. The frictional drag between plate and water is discussed in § 9.

5. Ripple formation under oscillatory water motion

The rolling-grain ripple. The relations between the sand-grain size and density, the repetition distance or pitch p of the ripple, and the elements ω and R of water motion producing it was complicated by the existence of at least two distinct types of ripple, each having its own formatory mechanism. Though the two ripple types may in some cases be similar in appearance, they differ greatly in character. The similarity in appearance between the two kinds of ripple, and between these and the profile of high-crested water waves is due respectively to the constancy of the angle of repose to which sand grains are tipped over the ripple crest in the two cases, and to the fact that this angle of a little over 30° makes at the crest, quite fortuitously, the precise angle of 120° which is the limiting angle of the water wave of greatest amplitude.

At the critical speed of the water motion at which grains on a smoothed surface first begin to move (see § 11), grains start to be rolled to and fro over the surface, but are not lifted off it. Since the grain movement is here confined to that phase of the stroke at which the relative water-sand velocity at the surface is greatest (which occurs at about quarter-stroke), the length of the grain path remains short. It lengthens, however, as the oscillation speed is raised.

Though initially distributed at random, the rolling grains become organized as time goes on, and tend to come to rest in parallel transverse zones. More grains reach these zones than leave them, so there is a progressive congregation of grains in them, and the zones soon become little wavy ridges a few grains high, whose crests sway from lee side to lee side during successive stroke reversals. Each lee side becomes a miniature scree at the angle of repose. As the ridge grows it shelters from the water action a wider and wider strip of flat surface on its successive lee sides; and when the sheltered area extends as far as the next ridge no further grain movement can take place anywhere but on the ridge itself. Hence, since the ridges can now collect no more grains, they cease to grow, and the arrangement becomes stable. The repetition distance is evidently the width of the flow shadow of the ridge, and depends on its height.

If the speed is raised, the increased water speed over the intervening flat strips sets more grains rolling, and these in turn become trapped whenever they reach a ridge. So the ridges grow again until a new state of stability is reached. Adjustment of the repetition distance between the ridges takes place by redundant ridges joining up and amalgamating.

The rolling-grain ripple occurs on all sands, but the profile varies. With fine grains the intervening surface remains flat. But with larger grains it becomes a nearly circular arc of large radius. The essential distinguishing feature of this type of ripple is, however, the entire absence of grain movement within the troughs, whose surfaces remain undisturbed either by water flow or by the impact to descending grains—for no crest grains leave the surface. The length-height ratio is evidently too big for the formation of the ripple vortex.

The rolling-grain ripple appears to be stable, for a given oscillation amplitude, between the critical speed of first movement on a smoothed surface and about double that speed, and within this range the vortex ripple will not form at all, provided there are no irregularities anywhere on the surface higher than say 20 grain diameters.

But if the speed exceeds twice the critical speed, the steep lee slopes reach such a height that an abrupt change takes place in the character of the water motion; the ripple vortex suddenly appears, and the whole regime breaks down.

The vortex ripple. The breakdown begins at one spot, where the crest happens first to exceed the critical height. From this spot the new regime of vortex ripples spreads rapidly over the rest of the surface like a disease. Successive stages are shown in figure 7, plate 3. Here the breakdown was started artificially by placing a small heap of sand, about 30 grain diameters high, on the surface. But any kind of surface feature will suffice—a pebble dropped on it, for instance, or a steep-sided dent made in it.

Indeed, it is not even necessary that the oscillation speed should have attained that needed for the spontaneous breakdown of the rolling-grain ripple. For the vortex-ripple mechanism will operate, and the ripples develop, from any sufficiently large surface feature at speeds even below that needed to start grain movement on a smoothed-out surface.

The operation of the vortex-ripple mechanism appears to be as follows. At the end of the stroke when the fully grown vortex begins to overrun the ripple, it comes into contact with the sand at the ripple's foot. Grains are scooped out from here and shot upwards parallel with the surface of the slope, as if the sand at the bottom had been touched by a spinning wheel. The path of the bulk of the lifted grains is such that they come to rest just at the crest of the ripple; and it seems to be this fact that maintains the ripple system in equilibrium and controls the size of the ripple.

With grains of a high terminal velocity of fall, none of them overshoot the crest into the water above, and there is therefore no suspended sand cloud. But with fine or with light grains a proportion of them get involved in the water of the vortex, and are carried up with it.

After the grains from the bottom have been lifted to the crest there is, except with very short strokes, a short pause till the vortex on its upward journey parallel with the ripple slope has passed the crest and become separated from the ripple altogether. By this time the ripple has just begun to move backward in the reverse direction. A jet of water now begins to squirt down the outward slope of the ripple, between the crest and the departing vortex. This jet flicks a volley of grains from the crest downwards parallel with the outward ripple slope. The grains impinge violently on the sand surface at the bottom, ricochet off it, scoring out a hollow where they strike, and finally come to rest beyond, where they gradually collect and build up the ridge of a second ripple.

As the return stroke proceeds no further grain movement takes place in the trough until the end of the stroke, when new vortices perform the same operation in the opposite direction. But during the stroke, while there is no large vortex in the ripple trough, the velocity of the water flow over the crest tends to flatten it by dislodging the grains at the sharp cusp and rolling them over down the lee side.

This velocity effect at mid-stroke becomes more pronounced as the stroke is made longer, so that the ripple height decreases. When the stroke length is very long and the velocity high the crests become so flat and rounded that the limiting wave-length/height ratio is reached at which the restoring end-of-stroke vortex cannot develop.

With very short strokes, on the other hand, there is no horizontal flow over the crest at any part of the stroke, and the crests remain sharply cusped, as in plate 3.

6. The pitch of vortex ripples

The first attempts to measure the pitch of the ripples gave inconsistent results because it was not realized that the ripples are capable of considerable compression when overcrowded. When generated directly from a smooth sand surface at speeds exceeding the breakdown value for the rolling-grain ripple (i.e. exceeding twice the critical speed), vortex-ripple nuclei are formed at several haphazard places at once. As each of these develop and multiply, the separate groups compete with one another for space; and the resulting pattern, though regular and apparently stable, has in reality a shorter pitch than would be the case if each ripple had adequate 'living room'. Thinning out can only occur if two ripple crests happen to incline towards one another and to coalesce. So, since the transverse arrangement seems to be very stable, accidental coalition can occur but rarely and one has to wait a very long time.

This elasticity is no doubt possible owing to the fact that each ripple ridge together with its alternate lee-side vortices comprises a complete unit capable of separate existence. At the true natural spacing the mean points at which the vortices scoop out grains from the bottoms and throw them up to the crests coincide with the centres of the troughs. Overcrowding merely results in these points being pushed off the trough centres towards the feet of the opposite ridges.

This uncertainty as to the true natural pitch was finally overcome by ensuring that the ripple system started from a single nucleus only. This was done by working at very low speeds—the critical speed for initial smooth-surface grain movement was taken as a standard—and by starting the ripple mechanism from a single artificially made transverse ridge. From this nucleus the ripples can multiply freely in both directions. The final natural pitch was assumed to have been attained when three adjacent ripples had grown to equal size. Ripples formed at higher speeds were started by the same method.

In all cases it was found that the pitch was independent of the speed of the oscillation. The experimental pitch measurements for sands of various grain diameters and densities are plotted in figure 1 against the oscillation amplitude R. A wide range of grain diameter and of grain density was used. The diameter varied between 0·25 and 0·009 cm., and the densities used were those of steel ($\sigma = 7{\cdot}9$), quartz ($\sigma = 2{\cdot}65$) and coal ($\sigma = 1{\cdot}3$).

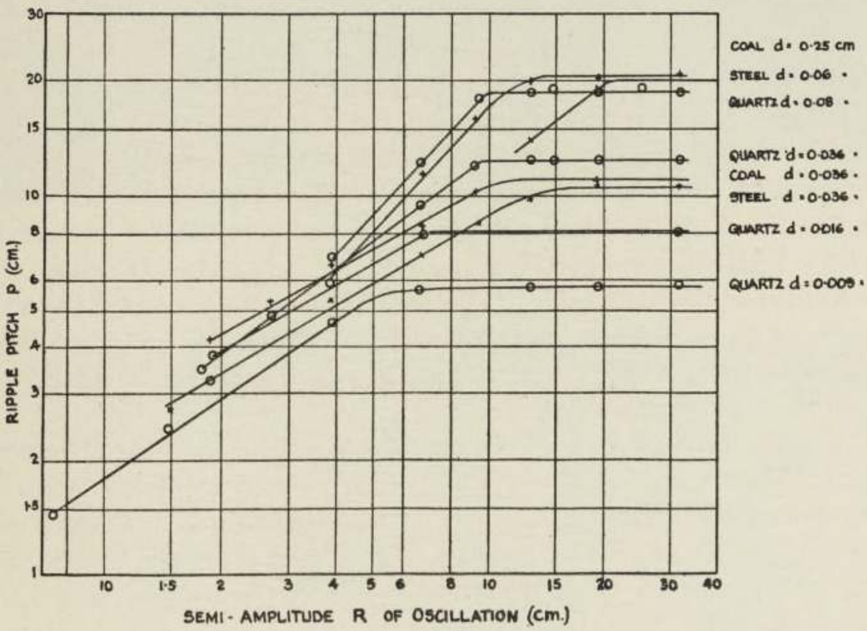

Figure 1

It will be seen that as the amplitude R of the stroke was decreased from the experimental maximum of 32 cm. the pitch p of the ripple, measured from crest to crest, remained constant at a value P which seems to depend only on the characteristics of the sand. But with the exception of the two biggest grain sizes, coal 0·25 cm. and quartz 0·08 cm., the pitch length began to fall suddenly as soon as the ratio R/P had reached unity, and for smaller values of R this ratio remained approximately constant.

From table 1 (in which values of P and d are given in cm.) it appears that the natural pitch P of the sand is independent of the grain density and varies nearly as the square root of the diameter. The range of values of ω and R for which the experimental values of P were found to hold extended from the lowest value of ω for initial grain disturbance, as given in § 11 up to the limits discussed in § 8.

TABLE 1

steel			quartz			coal		
d	P	$P/\sqrt{d}$	d	P	$P/\sqrt{d}$	d	P	$P/\sqrt{d}$
0·06	20·0	82	0·08	18·7	66	0·25	20·5	41
0·036	10·5	55	0·036	12·3	64·5	0·036	11·0	58
			0·016	8·0	63·5			
			0·009	5·8	61			

The above measurements were made on the pitch of ripples in sands of nearly uniform grain size. In order to test the effect on the pitch of non-uniformity of size, a quartz sand was made up in which the grades fell off very gradually on both the smaller and larger sides of the dominant diameter of 0·036 cm. It was found that although the size distribution was considerably wider than most sands found in nature, the ripple pitch still followed exactly the same curve as that for the uniform sand of 0·036 cm. diameter shown in figure 1.

The absence of any appreciable variation with the grain density is curious. Of the two most likely ways in which the diameter alone could become a controlling factor, surface roughness within the ripple trough and permeability of the material, there is a little evidence in support of the former. For in the case of the sand of mixed grain size which had the same value of P as that of the uniform sand of the dominant diameter, there was a distinct segregation of the grains; the hollow of the ripple was covered with those of the dominant size, whereas the smallest and largest grains collected together to form the crests.

The pitch/height ratio of vortex ripples reaches a minimum value of between 4·5 and 5 near the bend of the curves in figure 1. It increases as the amplitude is lengthened, till at the experimental limit of $R = 32$ cm. it had risen to nearly 8. The ratio appears to remain constant for shorter amplitudes, but at very short amplitudes measurement was complicated by the appearance in the ripple troughs of the features described in the next section.

7. The 'brick pattern' at very short stroke amplitudes

A curious modification of the vortex ripple appeared with all sands, independently of the working speed, when R was reduced to about $P/6$. Longitudinal and equidistant bridges were formed spanning the ripple troughs from crest to crest. The transverse spacing between them was very regular, being either one, two or three ripple pitches; and the positions of all the bridges across one ripple trough always 'broke joint' evenly with those across the troughs on either side, so that a perfect diagonal pattern was created. The effect is shown in figure 8, plate 4. Sometimes the bridges rose higher above the surface than the ripple crests themselves. The water

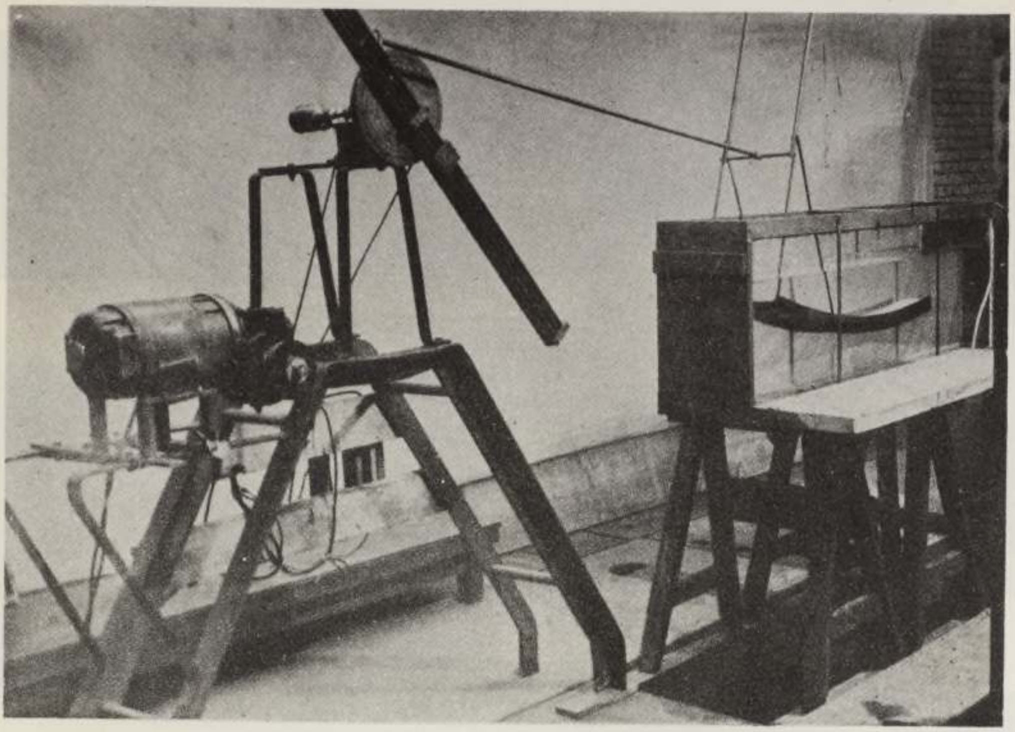

FIGURE 5 (*a*)

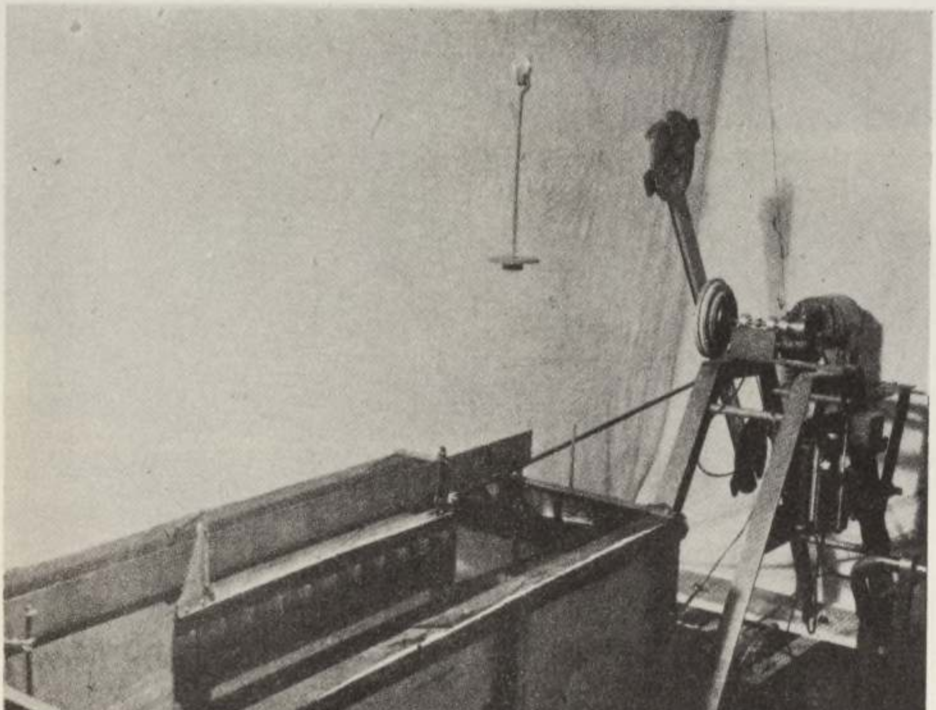

FIGURE 5 (*b*)

(*Facing p.* 8)

(*a*)

(*b*)

(*c*,

(*d*)

(*e*)

(*f*)

Direction of ripple	←	Ripple pitch	10 cm.
Half-period	3·4 sec.	Ripple height	1·5 cm.
Exposure	0·2 sec.	Stroke	20 cm.

FIGURE 6

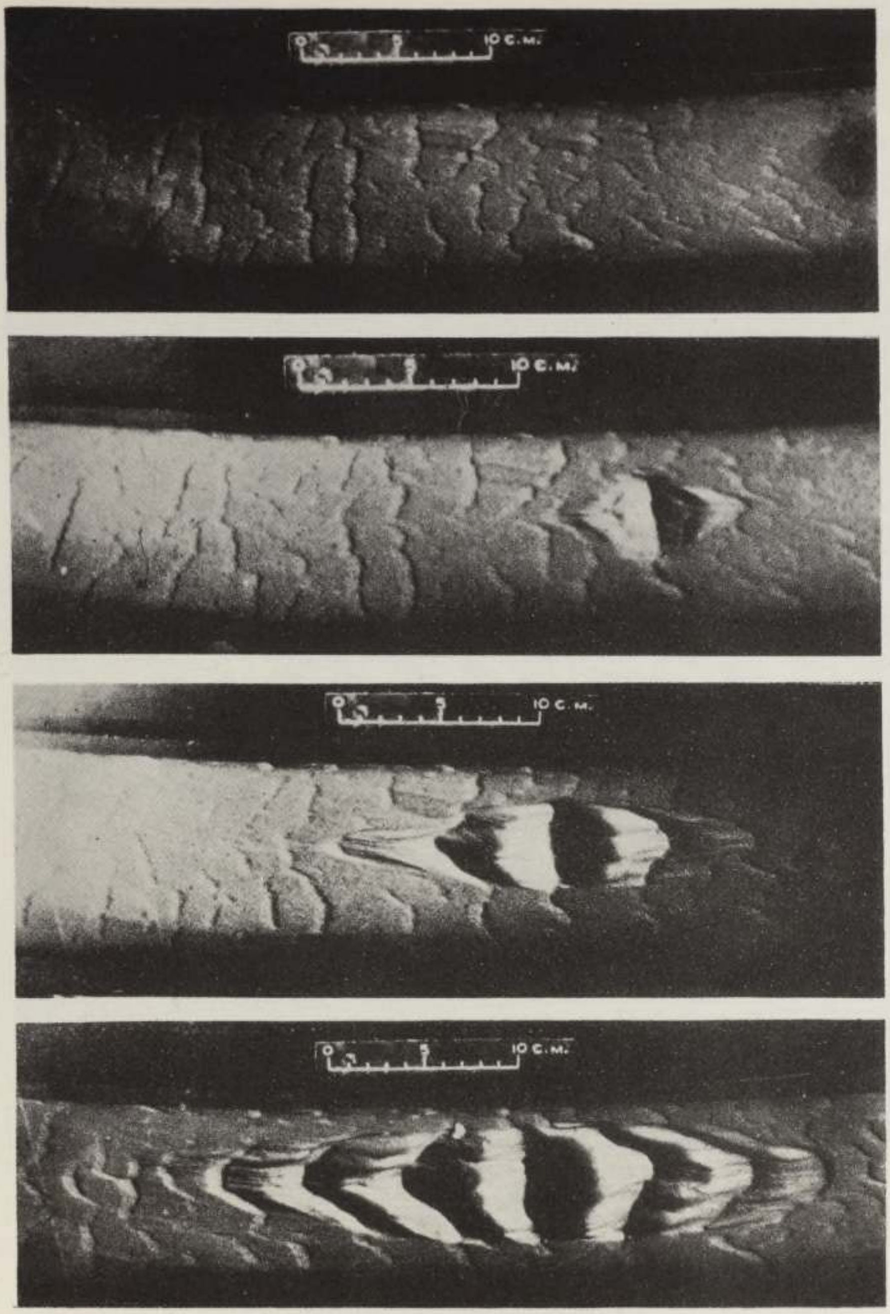

(*a*)

(*b*)

(*c*)

(*d*)

(*e*)

FIGURE 7

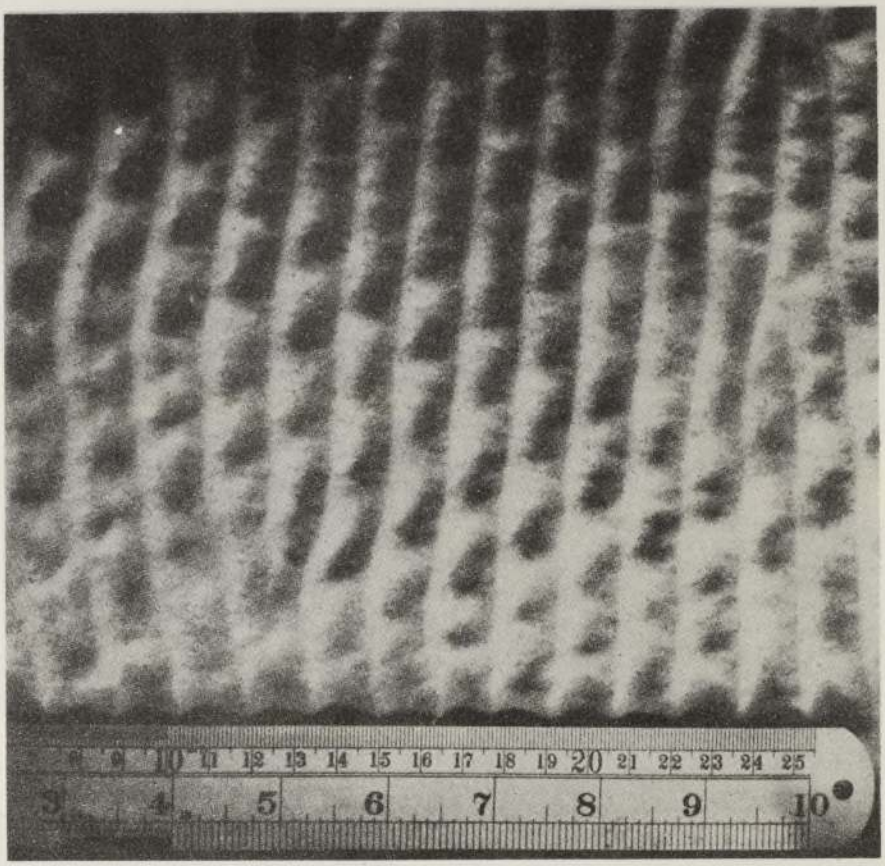

FIGURE 8

vortices must in these cases have been broken up into separate or nearly separate pieces, rather like strings of sausages.

The brick pattern appears in deep water on the sand bottom of a wave tank whenever the water amplitude is short enough; and the fact that it appears also under the very artificial experimental conditions where the bottom is oscillated through still water affords good evidence that no serious unrealities can be introduced by the experimental artifice. Further, the pattern persisted in the oscillating cradle even when the speed was raised to the theoretical breakdown value at which the end-of-stroke acceleration of the cradle must cause a general slipping of the sand grains, i.e. when $R\omega^2 = \mu g \dfrac{\sigma - \rho}{\sigma}$. This goes to reassure one as to the soundness of other experimental observations made close to this limit.

8. Physical limits to the existence of vortex ripples

Figure 2 gives a tentative schematic view of the various limits which appear from the experiments to bound the region (shown shaded) of water motion in terms of ω and R, in which the vortex-ripple mechanism can operate. Two examples have

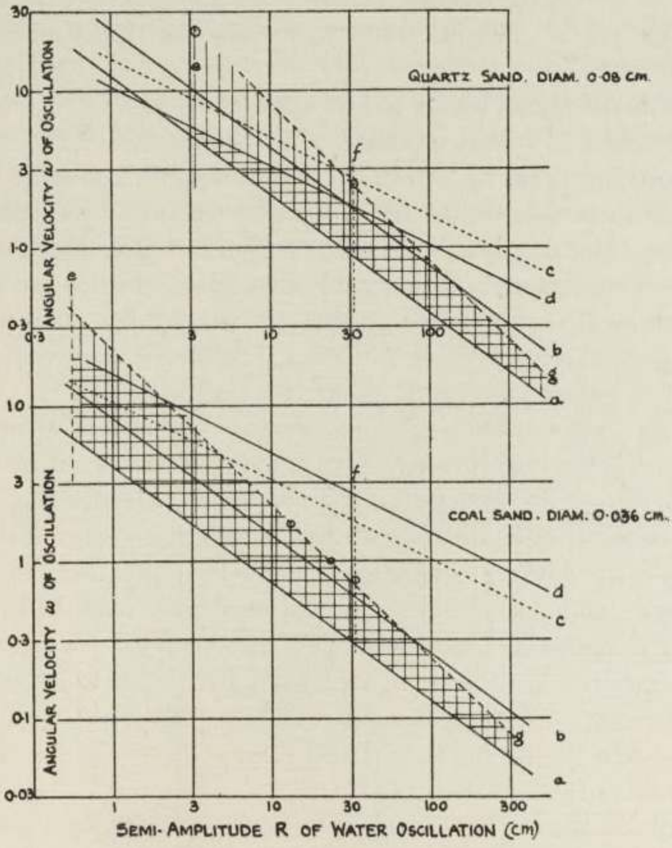

FIGURE 2

been taken: a quartz sand of 0·08 cm. diameter and a small grain coal sand of 0·036 cm. diameter. In the diagram each of the bounding lines shown is lettered as below. The limits for which there is direct evidence, either experimentally observed or calculated from wave theory, are shown as continuous lines. Inferred limits are shown as broken lines and limits set only by the apparatus used are dotted.

(*a*) Critical water motion for first disturbance of a smoothed-out sand surface. This was found experimentally, and is given by equation (4) in § 11, where it is further discussed.

(*a'*) Motion at which the vortex mechanism will continue to operate when once one ripple is formed. Speeds about 20 % lower than (*a*) (omitted from figure 2 for sake of clarity).

(*b*) Spontaneous formation of vortex ripples when no initial surface feature is present as a nucleus. Speeds about twice (*a*).

(*c*) Artificial limit set by experimental method, whereby the cradle acceleration $R\omega^2$ could not exceed $\mu g \frac{\sigma-\rho}{\sigma}$, where μ is the friction coefficient.

(*d*) Limit of bottom-water accelerations possible under stable travelling water waves. About $g/6$.

(*e*) Limit set to the smallest ripple pitch by size of the grain. This could only be observed for large grains. Ripples failed to form when ripple pitch was less than 30–50 grain diameters.

(*f*) Limit of stroke length; set by size of apparatus only.

(*g*) Observed failure of vortex mechanism at long strokes.

The lower speed limits set by (*a'*) or (*b*) will be seen to converge with (*d*) as the stroke amplitude decreases. Since both (*a'*) and (*b*) shift upwards with increase of either grain diameter or grain density, the region in which large heavy grains can ripple under free water waves is considerably restricted. But (*d*) can be raised under special conditions such as the violent oscillations which take place at the foot of a vertical wall against which waves are breaking. I obtained steep well-formed ripples by this means with pebbles 0·9 cm. in diameter (Bagnold 1940).

The limit (*g*) for long strokes is of some practical interest. Unfortunately, it lay in most cases beyond the experimental limit (*f*) of $R = 32$ cm. set by the apparatus, or else so close to the acceleration limit *c* as to be of doubtful significance. There was, however, fairly definite evidence that at high speeds the vortex mechanism began to fail in the case of the 0·08 cm. quartz sand before the stroke amplitude reached the experimental limit; and that failure occurred at shorter strokes as the grain size and/or density was reduced. The characteristic steep-sided vortex ripple, with its plume of whirling grains, gave place to a very flat streamline undulation over which a dense layer of moving grains glided low and smoothly like an oily liquid. There was also evidence of a change of pitch. In the case of the 0·036 cm. coal sand it rose abruptly from 11 to 15 cm.

Since the disappearance of the vortex occurs first at the highest oscillation speeds and longest strokes, it would seem to be a velocity effect; an inference which is supported by the three limiting values found for ω in the case of the fine coal sand of 0·036 cm. diameter, and plotted in figure 2*b*. If so, it can be represented by a 45° line in the diagram.

9. Magnitude of the oscillatory drag of a rippled surface under waves

In experiment 2, figure 5*b*, the mean drag τ per unit area of the artificially rippled plate was obtained from the measurement of the work done per oscillation in moving the plate through the water. For each of a range of different semi-amplitudes R, from 30 to 5 cm., records were made of the final steady angular speed ω maintained by each of a series of weights. The work done was given by the product of the effective weight (corrected for mechanical friction) and the distance it had fallen (the drum circumference). From this the mean drag τ throughout the oscillation was found by dividing by the total distance $4R$ travelled by the plate and by the area of the plate, both sides of which were rippled. In order to check for possible end-effects, the experiment was repeated with a short plate carrying one ripple only. The results of this check showed that end-effects were negligible.

The pitch/height ratio of the ripples was 6·7 to 1; and the ripple trough sections consisted of circular arcs meeting to form sharp crests at an angle of 120°. Two plates were used, on one of which the ripple pitch was 10 cm. and on the other twice the size.

The resulting figures for τ and ω for various values of R are plotted in figure 3. τ was found to be proportional to ω^2 for all values of R. But the variation of τ with R and with the ripple pitch p appeared to follow two different laws according to whether R was greater or less than p.

For all values of R/p less than unity, the drag coefficient $k = \tau/\rho\omega^2R^2$ was constant and independent of the ripple pitch, and thus

$$R/p < 1, \quad k = 0{\cdot}08. \tag{1}$$

Corroboration of this result seems to be forthcoming from steady-flow considerations. The drag, per plate, of a 'venetian blind' of a series of flat independent and widely spaced plates set at right angles to the direction of motion is $c\rho v^2A$, where A is the area of the plate and c depends on its length/breadth ratio. For infinitely long plates the value of c is given as 2 in *Smithsonian Tables*, Washington, 1934, table 159. Hence, if the breadth of each plate is $2h$, and their spacing is p, the drag coefficient per unit distance in the direction of motion is $2 \times 2h/p$. If now the plates are connected by a plane membrane through their central axes, each side becomes a surface roughened by transverse slats of height h, and the drag coefficient k for one side only will be $2h/p$. Assuming (i) that one can compare this with the r.m.s. velocity in the oscillating case, i.e. that it should be halved in order to become the k of equation (1) for which the maximum velocity $R^2\omega^2$ was used, and (ii) that the wide spacing in the steady flow case is comparable with the short stroke in the oscillating case, then, giving h/p its experimental value of 1·5/10,

$$k = 0{\cdot}15. \tag{1a}$$

This is of the same order as the experimental value, and is also independent of R. That it should be too big is to be expected, since the slats were vertical whereas the ripple troughs were filled in by smooth curves.

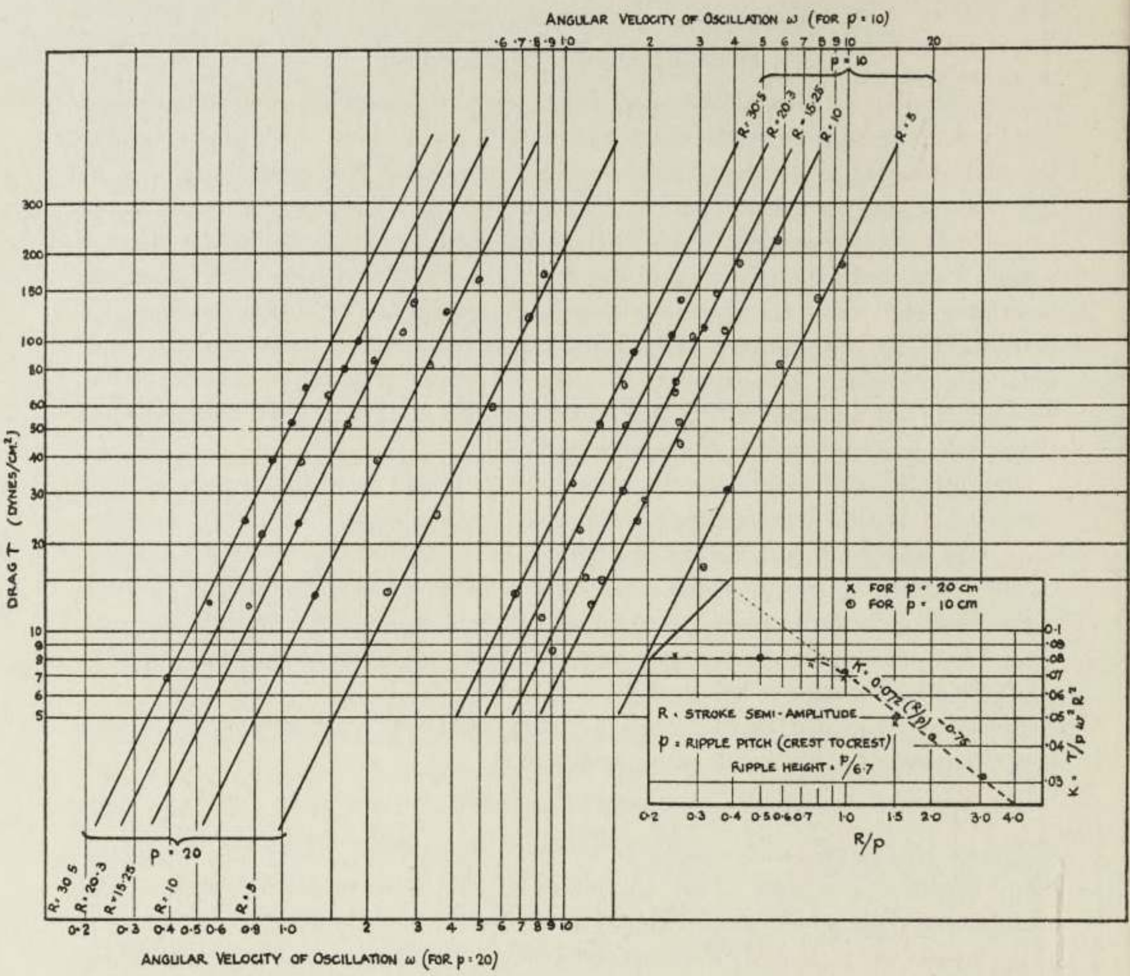

FIGURE 3

For values of R/p greater than unity, the experimental drag falls off with increasing values of R according to

$$R/p > 1, \quad k = 0{\cdot}072\left(\frac{R}{p}\right)^{-0{\cdot}75}, \tag{2}$$

though to what extent the numerical constant depends on the ratio h/p is not known.

In this case it is necessary to deal with the formation of a succession of transitory boundary layers, and confirmation of the results again comes from the steady flow case. Now I. Moyal, in an unpublished Ph.D. thesis,* found that the drag

* University of London, 1935.

coefficient of a rough plate of length L moving longitudinally through the water is given by

$$1/\sqrt{k_1} = 4{\cdot}65 \log\left(\frac{2L}{d} \times 1{\cdot}64\right), \tag{3}$$

where d is the diameter of the sand grains with which the surface was roughened; and H. Schlichting (1936) gives values of the sand diameter d which is equivalent to the heights of other sorts of roughness. For vertical transverse slats of height h spaced at $p = 7h$, d is about $14h$.

Assuming that for the length L of the plate may be substituted the amplitude $2R$ of the oscillation, and putting $d = 14 \times 0{\cdot}15 \times p$, equation (3) becomes

$$1/\sqrt{k} = 4{\cdot}65 \log 3{\cdot}15 \frac{R}{p}. \tag{3a}$$

For $R/p = 1$ this gives $k = k_1/2 = 0{\cdot}09$, which may be compared with the experimental value of $0{\cdot}072$. For $R/p = 3$ it gives $k = 0{\cdot}025$, which is rather smaller than the experimental value of $0{\cdot}03$ to be found from figure 3. There is, therefore, a general agreement as regards the values of k, and k does fall off as R increases, though the log relation yields in this region of R/p a rather steeper curve.

10. Relations between drag results and dimensions of actual sand ripples

In attempting to relate the above results to those of the preceding sections, it should be borne in mind that:

(a) The final curve of figure 3 applies only to ripples of constant pitch/height ratio $\phi = p/h$, whereas in the actual sand ripple ϕ increased as a direct function of R, of the order of $(R/p)^{0{\cdot}25}$ for all observed values of R/p greater than unity.

(b) The limiting value of ϕ which the sand ripple attains where R/p is reduced to unity is doubtless set by the almost constant angle of repose of the sand grains on the sides of the ripple crest, and by the curvature of the trough bottom which could hardly have a radius less than that of the vortex which sweeps it out.

(c) With two exceptions, probably created in both cases by the excessive sharpness of the grains, R/p does not appear in actual sands ever to be able to fall much below unity, so it is possible that equation (1) never operates, because of the limiting value of ϕ being reached.

Now the whole phenomena of the vortex ripple suggests that when $R/p > 1$ there is a conflict between the end-of-stroke retardation, which appears to be responsible for the vortex which heightens the ripple crest, and the mid-stroke velocity of flow which tends to flatten out the crest; and the ratio retardation/velocity is $1/R$. Since from (a) above it seems that the actual value of k varies much more nearly as p/R than $(p/R)^{0{\cdot}75}$, it looks as if the 'natural pitch' P is such that

$$k \propto P \times \frac{\text{retardation}}{\text{velocity}},$$

and as if for any given grain diameter and stroke length the sand so adjusts itself as to give the maximum possible drag allowed by (i) the ratio retardation/velocity, (ii) the grain diameter of the sand, and (iii) the limiting geometry of the ripple.

11. Smooth sand surfaces. The critical water motion for first disturbance of the grains

The sand sample was spread over the cradle of experiment 1, figure 5*a*, and the surface carefully smoothed. The oscillation speed was then raised till grain movement began.

An outstanding feature in this experiment was the absence of any signs of turbulence in the water, even at distances above the surface comparable with one grain diameter. The skein of colour threaded through the water which was left by a particle of dye as it fell to the bottom remained almost undisturbed after many oscillations had taken place.

For each of the sands used the values of ω corresponding to various semi-amplitudes R of the oscillation are plotted in figure 4, whence the critical angular speed ω appears to conform with the empirical relation

$$\omega = 21{\cdot}5R^{-0{\cdot}75}\gamma^{0{\cdot}5}d^{0{\cdot}325}, \tag{4}$$

where γ is the ratio $\dfrac{\sigma-\rho}{\rho}$ of apparent density, σ the density of the material having the values given in § 7, and ρ being unity for water.

In these measurements it is unlikely that the unreal conditions of still water and an oscillating cradle can have affected the results, since in this case the maximum accelerations of the moving cradle at the end of each stroke were very small compared with the limiting value of $\dfrac{\sigma-\rho}{\sigma}\mu g$; and, moreover, the initial grain movement took place at a later phase when the acceleration was considerably less than the maximum.

But there are several sources of possible error common to all measurements of the fluid velocity for first-grain movement:

(*a*) The difficulty of maintaining by eye, from one amplitude to another, and from one grain size to another, a consistent standard as to the proportion of moving grains on the surface which should constitute 'first movement'. This may well have introduced a systematic error which would affect the exponent of R, and would increase in magnitude as the stroke was shortened.

(*b*) The impossibility of using completely uniform material. The first surface grains to move might have been those of exceptional size or shape.

(*c*) In the case of the lightest material (coal) the possibility that the first grains to move might have had tiny air bubbles adhering to them. This error was watched for, but may not have been entirely excluded. Hence the actual value of γ in this case may have been rather too high.

With the justifiable introduction of g in association with γ in the form $(g\gamma)^n$, (4) may be written as

$$\omega = A R^{0.75} (g\gamma)^{0.5} d^{0.25} d^{0.075}, \tag{4a}$$

which is non-dimensional except for the final remnant exponent of d. But it seems likely from the apparent absence of turbulence that (4a) should also contain a factor involving the viscosity ν.

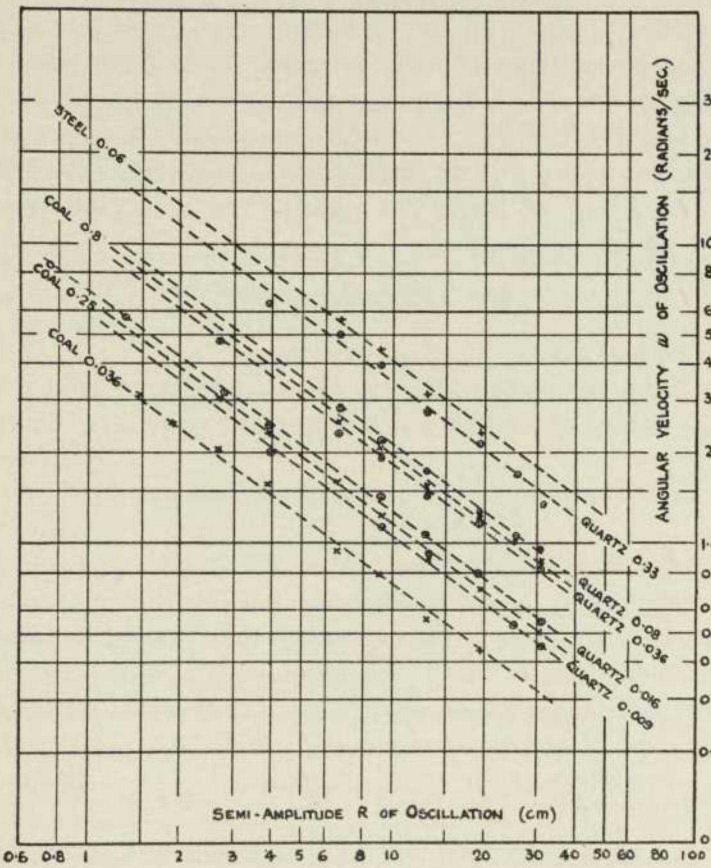

FIGURE 4

Further experiment is needed, using fluids of other viscosities, but (4) may be of some use as a first approximation in interpreting the results of model experiments with low-density artificial sands.

The above work was carried out on behalf of the Ministry of Supply, and my thanks are due to the Director-General of Scientific Research and Development for permission to publish.

REFERENCES

Bagnold 1940 *J. Instn Civ. Engrs*, **15**, 27.
McCowan 1891 *Phil. Mag.* **32**, 45.
Schlichting 1936 *Werft, R. Hafen*, pp. 99–102.

Note on R. A. Bagnold's empirical formula for the critical water motion corresponding with the first disturbance of grains on a flat surface

By Sir Geoffrey Taylor, F.R.S.

In §11 of his paper Bagnold calls attention to the fact that at the stage when oscillating water is just beginning to move sand grains no turbulence is produced even at a distance from the surface comparable with one grain diameter. The motion of water near a smooth plate which is oscillating horizontally has been calculated (Lamb 1932). In Bagnold's notation the horizontal velocity u of the water at height y above the plane is

$$u = \omega R e^{-\beta y} \cos(\omega t - \beta y), \tag{1}$$

where $\beta = \sqrt{(\omega/2\nu)}$ and ν is the kinematic viscosity.

At distances from the plate which are small compared with $1/\beta$ the motion is nearly the same as that of a liquid which is shearing uniformly at rate α, where

$$\alpha = \left[\frac{\partial u}{\partial y}\right]_{\eta=0} = \nu^{-\frac{1}{2}}\omega^{\frac{3}{2}} R \cos(\omega t + \tfrac{1}{4}\pi). \tag{2}$$

In fact, the motion through the whole layer which extends from the surface to $y = \sqrt{(2\nu/\omega)}$ is very nearly a uniform shearing flow, so that it seems justifiable to consider cases where grains have diameters less than $\sqrt{(2\nu/\omega)}$ as though they were being subjected to the stresses which would be applied to their surfaces by a uniform shearing motion in the fluid. In Bagnold's experiments ω varied from 0·5 to 6 sec.$^{-1}$, so that taking $\nu = 0{\cdot}011$ the above consideration might be expected to apply to grains whose diameters were below the range $\sqrt{\dfrac{2(0{\cdot}011)}{0{\cdot}5}} = 0{\cdot}2$ to $\sqrt{\dfrac{2(0{\cdot}011)}{6}} = 0{\cdot}06$ cm. Three grades of quartz sand used by Bagnold satisfied this condition, namely, those of mean diameter 0·0016, 0·016 and 0·036 cm. diameter.

The system of flow patterns produced in a uniformly shearing fluid by a grain of given shape when the diameter, d, the rate of shear α or the kinematic viscosity ν vary depends on a single variable only, namely the Reynolds number

$$z = \alpha d^2/\nu, \tag{3}$$

and the force which the fluid exerts on the grain must be of the form

$$F = d^2\rho(\alpha d)^2 f(z), \tag{4}$$

where f is a function which depends on the grain shape only and not on its dimensions. The condition that the grain will move must therefore be of the form

$$\rho\alpha^2 d^4 f(z) = A(\sigma - \rho) g d^3, \tag{5}$$

where A is a constant depending on the grain shape only. (5) may be rewritten in the form

$$\frac{\gamma g d^3}{\nu^2} = \frac{1}{A} z^2 f(z), \tag{6}$$

where

$$\gamma = \frac{\sigma - \rho}{\rho}. \tag{7}$$

(6) may now be regarded as an equation for (z) and can be solved to give

$$\frac{\alpha d^2}{\nu} = z = \phi(\zeta), \tag{8}$$

where

$$\zeta = \frac{\gamma g d^3}{\nu^2}. \tag{9}$$

In this form (8) may be compared with Bagnold's empirical equation (4) § 11 which gives the way in which ω depends on R, d and γ for substituting the maximum value of α from (z), namely $\alpha = \nu^{-\frac{1}{2}}\omega^{\frac{3}{2}} R$, (8) becomes

$$\omega = R^{-\frac{2}{3}} \nu d^{-\frac{4}{3}} \chi\left(\frac{\nu g d^3}{\nu^2}\right), \tag{10}$$

where $\chi(\zeta) = [\phi(\zeta)]^{\frac{2}{3}}$.

It will be seen that this analysis leads to the expectation that the exponent of R will be $-0{\cdot}66$ instead of the empirical value $-0{\cdot}75$.

The particular form of χ which most nearly coincides with Bagnold's empirical relation is $\phi(\zeta) = B\zeta^{\frac{5}{6}}$. This gives

$$\omega = (\text{constant})\, R^{-\frac{2}{3}} (g\gamma)^{\frac{5}{9}} \gamma^{-\frac{1}{9}} d^{\frac{1}{3}}, \tag{11}$$

making the exponent of $g\gamma$, $0{\cdot}45$ instead of the empirical $0{\cdot}5$; and that of d, $\frac{1}{3}$ instead of $0{\cdot}325$.

It is of interest to note the two limiting forms which might be expected when $\alpha d^2/\nu$ is very small or very large. In the former case (Stokes' law), $f(\alpha d^2/\nu)$ is proportional to $\nu/\alpha d^2$ and (10) reduces to

$$\omega = (\text{constant})\, R^{-\frac{2}{3}} (g\gamma)^{\frac{2}{3}} \nu^{-\frac{1}{3}} d^{\frac{2}{3}} \quad \left(\text{Stokes' law, small values of } \frac{\alpha d^2}{\nu}\right), \tag{12}$$

while in the latter

$$\omega = (\text{constant})\, R^{-\frac{2}{3}} (g\gamma)^{-\frac{1}{3}} \nu^{\frac{1}{3}} d^{-\frac{1}{3}} \quad \left(\text{constant drag coefficient, large values of } \frac{\alpha d^2}{\nu}\right). \tag{13}$$

It seems from (11) that the empirical formula gives exponents for γ and d which are intermediate between those of (12) and (13) but, so far as the variation of ω with d is concerned, the empirical formula is much closer to the Stokes' law limit (equation (12)).

It is of interest to make a rough approximate calculation of the critical value of α at which grains might be expected to begin to roll. Taking the case of a cubical grain of side d, if the tangential traction on the upper face due to viscous drag is the same as that on the surface on which the grain rests, it will give rise to a moment about the down-stream lower edge of the cube of amount $\mu\alpha d^3$. The face of the cube which faces the stream might be expected to experience a pressure of approximately the same magnitude as that in a half pitot tube placed facing the stream. This has been measured (Taylor 1938) and found to be approximately $1{\cdot}2\mu\alpha$ when the opening of the tube is so small that Stokes' law is obeyed. If the rear face of the cube has a suction of this magnitude, the moment of the normal components on the front and rear faces about the lower edge is $1{\cdot}2\mu\alpha d^3$. It seems likely that the normal component on the top face and the tangential components on the front and back faces will contribute less than the components already mentioned. The tangential drag on the side faces will make some positive contribution towards upsetting the cube, but it is difficult to make an estimate of its magnitude. These considerations lead to the conclusion that a cubical grain might be expected to roll when

$$2{\cdot}2\mu\alpha d^3 > \tfrac{1}{2}(\rho-\sigma)\,gd^4, \tag{14}$$

or expressed in terms of ω and R if

$$\omega > (4{\cdot}4)^{-\frac{2}{3}}\,(\gamma g)\,\tfrac{1}{3}\nu^{-\frac{1}{3}}R^{-\frac{1}{3}}d^{\frac{2}{3}}. \tag{15}$$

If this calculated value of ω is represented by the symbol ω_{cube}, the following table gives a comparison between ω_{cube} and the observed value of ω at which grains begin to move ($\omega_{\text{obs.}}$) taken from Bagnold's figure 4.

d (cm.)	R (cm.)	$\omega_{\text{obs.}}$ (sec.$^{-1}$)	ω_{cube} (sec.$^{-1}$)
0·009	11	1·0	2·0
0·016	8	1·5	3·63
0·036	10	1·8	5·4

It will be seen that $\omega_{\text{obs.}}$ and ω_{cube} are of the same order of magnitude, but that $\omega_{\text{obs.}}$ is greater than ω_{cube}. If similar rough arguments had been applied to the case of a hexagonal grain of height d in which the moment of the gravity component about the rolling edge is (volume of grain) $(\rho-\sigma)\,g\left(\dfrac{d}{2\sqrt{3}}\right)$ instead of $\left\{(\text{volume})\,(\rho-\sigma)\,g\left(\dfrac{d}{2}\right)\right\}$, better agreement between the calculated and observed values of ω would have been obtained.

References

Lamb 1932 *Hydrodynamics*, 6th ed. p. 620. Camb. Univ. Press.
Taylor 1938 *Proc. Roy. Soc.* A, **166**, 479.